Multi-objective Sizing Optimization of Borehole Heat Exchangers

Seung-Hoon Park[1], Byung-Ki Jeon[1], Yong-Sung Jang[2], Eui-Jong Kim[1*]
[1]Department of architectural engineering, INHA University, Incheon, South Korea
[2]GS E&C, Seoul, South Korea
Contact information: ejkim@inha.ac.kr

ABSTRACT

Adequate sizing of borehole heat exchangers (BHE) is crucial for successful design of the ground-coupled heat pump (GCHP) system. Very recently, simulation-based sizing methods have been proposed using an optimization tool and the TRNSYS duct storage (DST) model. Other than existing BHE models, the DST model can describe the bore field by setting fewer parameters, apt for optimization. However, the DST model cannot account for irregular BHE arrangements which are common in many projects. In this work, the *L*-shape bore field is simulated with the DST model by modifying a DST parameter. Varying design entering water temperatures, several optimal sets of design variables such as the spacing, number of boreholes, and unit length are calculated, which form Pareto solutions. Each point on the Pareto curve indicates a possible sizing solution. This new sizing method provides an amount of information that is useful for a decision process.

INTRODUCTION

Ground-coupled heat pump (GCHP) systems are regarded as a renewable energy system. However, the important initial cost is still an obstacle to steady growth. Proper sizing of borehole heat exchangers (BHE) is crucial in order to reduce the initial cost while guaranteeing higher system performance than conventional systems.

In general, sizing methods are based on the different ground load pulses: peak, monthly, and annual types (Kavanaugh, 1995). Thermal effects of these pulses on the ground are variable depending on the bore field configuration and the total BHE length. Undersized BHEs may cause the system failure while oversized systems lead to the increase of initial cost. With varying BHE arrangements, adequate length can be found when the maximum or minimum entering water temperatures (EWT) to heat pumps are close enough to a design EWT(EWT_{SET}).

Ahmadfard et al. (2016) reviewed that several studies have been conducted to investigate the effects of variable EWTs over the design period on sizing results. The time-variable EWTs, one of the most important parameters in the GCHP system, affect the whole system efficiency during the long-term operation (Park et al., 2016), and it is also necessary to perform more accurate sizing. If the load side conditions are constant, the COP of heat pumps is mostly affected by the EWT, and it decides the ground loads.

On the other hand, the duct storage (DST) model, one of the well-known BHE models, developed by Hellström (1989), performs the hourly calculation of the EWTs for a regularly-placed cylindrical bore field configuration. This DST model is provided in the TRNSYS library as Type 557. Recent studies proposed a new sizing method by using DST model combined with optimization program GenOpt (Ahmadfard et al., 2016) and (Park et al., 2016). When the DST model is used for BHE sizing, only the cylindrical bore field configurations are accounted for. However, a previous study has shown that the DST model for irregular borehole configuration can be achieved by modifying a ground heat storage volume (Bertagnolio et al., 2012). Our work adopts a similar approach to apply the DST model in irregular arrangements.

In this study, the DST-based TRNSYS simulation and MultiOpt tool are coupled. The MultiOpt tool uses Multi-objective algorithm, NSGA-II (Non dominated Sorting Genetic Algorithm), to find multiple optimal results that are placed on the Pareto-front (Deb et al., 2002). This optimizing method aims that their objective functions are to be minimized. Minimizing annual energy consumption of heat pumps and initial cost are set as our objective functions. Each simulation is run with a random EWT_{SET} selected within a user defined EWT range, optimization constraints, possible numbers of BHE, and a possible unit-length range.

PREVIOUS STUDIES

This section brifly describes the DST model and the previous work of Bertagnolio et al. (2012).

The DST model accounts for the heat transfer between boreholes and ground under the pre-defined borehole configuration as shown in Figure 1. Since the DST model assumes boreholes arrangement as regularly placed

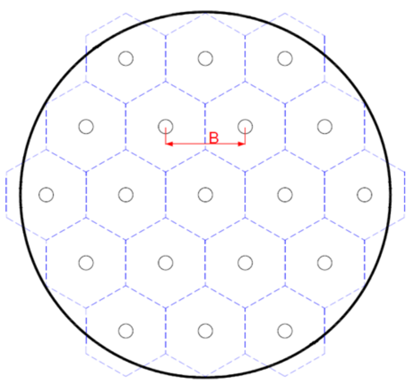

Figure 1: Schematic of the BHE configuration in the DST model (19 boreholes case).

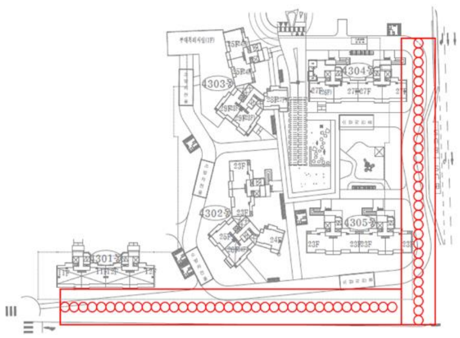

Figure 2: Common BHE configuration in Korea.

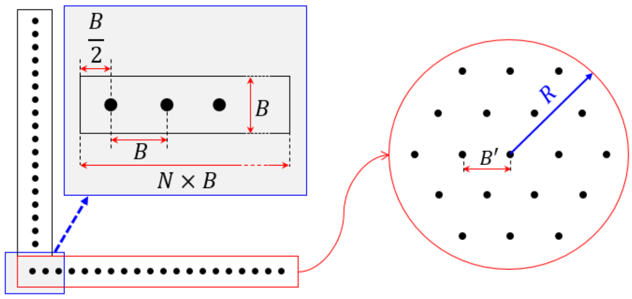

Figure 3: Proposed method for modifying V_{DST}

cylindrical configurations, the simple parameter V_{DST} (ground heat storage volume) can explain the borehole configuration. The smaller the parameter is, the closer the boreholes are placed for the same number of boreholes. The DST model automatically locates boreholes and calculates the storage volume, when users set borehole spacing (B), unit borehole depth (H) and the number of boreholes (N) as Equation (1).

$$V_{DST} = \pi \times N \times H \times (0.525 \times B)^2 \qquad (1)$$

When B is constant, the EWT calculated by the DST model (EWT_{DST})is a function of the total length $L(=N\times H)$. Therefore, an optimization tool can contol the EWT_{DST} over a design period close to the EWT_{SET} by varying N, H or B.

According to previous studies, it is possible to size BHEs in TRNSYS using the GenOpt tool. Advantages of this simulation-based optimization for design are summarized as follows:

- It accounts variable COP values for sizing borehole heat exchanger (Ahmadfard et al., 2016).
- The same TRNSYS simulation project can be used both sizing and detailed engineering (Park et al., 2016).
- Dynamic building and ground load with their peak loads are directly taken into account without assumptions.

In this work, we attempt to use such a sizing method for irregular BHE configurations. As with the case of Capozza et al. (2015), BHE configurations are composited by buildings layout. Conventionally, In Korea, the high-density buildings adopt the *L*-shape BHE configurations as shown in Figure 2. Therefore, a modification method of V_{DST} to account for the *L*-shape BHE configurations is required.

As mentioned in the introduction, Bertagnolio et al. (2012) were the first to mention the possibility of using DST for irregular borehole configurations. Especially, the simulation result of *I*-shape borehole configuration was approximatly fitted compare to hybrid ground heat exchanger model. Based on this relevance, this study also compared EWT_{DST} with hybrid reduced (HR) model (Kim et al., 2014), which is available a describtion of detailed bore field, under *L*-shape borehole configuration.

MODIFYING DST STORAGE VOLUME

Bertagnolio et al. (2012) mentioned EWTs of *I*-shape bore field can be calculated using a modified V_{DST} . The lower portion of Figure 3, representing *I*-shape BHE configuration, explains how to modify the V_{DST}. According to their approximation, the perimeter of red-colored *I*-shape area is almost equal to the cylindrical cross sectional perimeter in the original DST configuration as given in Equation (2). And they compared this adjusted DST model with the *g-function* of hybrid cylindrical heat source model. This is a so-called rule-of-thumb evaluation, but it allows for modifying V_{DST} for irregular configurations by using eqivalent ground heat storage volume of DST model($V_{DST\text{-}modif,\,I}$).

$$2\pi R = 2\times([N\times B] + B) \qquad (2)$$

$$V_{DST-modif,I} = \pi \times H \times \left[\frac{(N\times B) + B}{\pi}\right]^2 \qquad (3)$$

Equation (3) represents $V_{DST\text{-}modif}$ deduced from Equation (2) for the *I*-shape BHE configuration. In this work, this approximation is applied to the *L*-shape borehole configuration (see Figure 2). We assume that the *L*-shape bore field is composed of two *I*-shape bore field volumes as Figure 2. The main assumption of the *L*-shape bore field is that the thermal interference between two *I*-shape bore field is not accounted for.

$$V_{DST-modif,L} = s \times \pi \times H \times \left[\frac{\left(\frac{N}{s}\times B\right) + B}{\pi}\right]^2 \qquad (4)$$

Equation (4) is a modification of the approximation metioned by Bertagnolio et al. (2012) to interpret the *L*-shape irregular bore field. Here, the s means the number of *I*-shape bore field. In the case of *L*-shape in Figure 2, s is set to 2. For a *U*-shape case, s may become 3. To verify this assumption, the DST model is compared to the

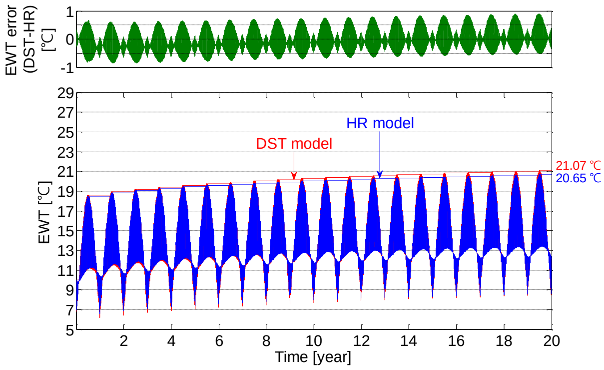

Figure 4: EWT difference between DST model and HR model.

HR model (Kim et al., 2014) for the case of 19 boreholes, respectively 100 m deep. The HR model uses a modified g-function generated for any types of bore field, so it is apt for describing irregular BHE configurations.

For this comparison, the ground load is cooling dominant which annual peak cooling load is 4.4 kW and annual peak heating load is 2.3 kW per borehole. The total ground load scale is about 24 RT, and boreholes is 5 m apart. Other parameters used for this comparison are the same as the simulation conditions used for the case study (see Table 2).

The comparison results are given in Figure 4. The top graph of Figure 4 shows the error between the DST model with $V_{DST\text{-}modif,L}$ and the HR model, and the bottom one gives the EWT evolution over the period. The maximum error in EWT between the models is less than 1 °C during a 20 year simulation, and the EWT difference is only 0.42 °C at the end of the simulation, a target peorid for sizing. Acconding to Kim et al. (2014), this error is partly caused by capacity effects as the DST model do not account for the thermal capacity inside boreholes. Another reason of this error is seemingly that the thermal interferences between two *I*-shape bore fields are ignored for $V_{DST\text{-}modif,L}$ and the $V_{DST\text{-}modif,I}$ for the *I*-shape bore field is also an approximation. This error in EWTs will be increased for the cases of large numbers of boreholes, large ground loads, or highly dominant ground loads where thermal interferences effects are more important. Therefore, thermal interference effects among boreholes are accounted for in a more detailed way for describing irregular configurations with the DST model.

OPTIMIZATION METHODOLOGY

Optimization method can be categorized into several groups (Goldberg, 1989). Among them, calculus-based methods and stochastic methods have being used in order to get optimal solutions (Magnier et al., 2010), (Chantrelle et al., 2011) and (Asadi et al., 2012). A similarity of both methods are found in defining objective functions and design variables.

Calculus-based methods have been widely used for mono-objective optimization. For instance, the GenOpt (Wetter, 2001) program was developed to determine the optimal design parameters under a given single objective function. The GenOpt is easily combined with transient simulation programs (Ahmadfard et al., 2016), (Asadi et al., 2012) and (Park et al., 2016). However, this method can not cover the multicriteria optimization.

A well-known method of the stochastic group is the genetic algorithm (GA) (Holland, 1975). This algorithm was introduced based on an analogy of the selection strategy in nature. From the GA, multi-objective evolutionary algorithms (MOEAs) were proposed over the past decades in order to optimize the complex system parameters under multicriteria problems. MOEAs are able to run optimization with multiple objective functions, and they can provide non-dominated Pareto solutions (Magnier and Haghighat, 2010). However, these algorithms require an important computational resources to sort dominated values in every generation. This is time consuming when population sizes are large.

The NSGA-II (Deb, 2001) calculates a crowding distance that represents relevancy of each population gererated at every generation. This is able to maintain a better spread of soluions and converge better in the obtained Pareto-front compared to other MOEAs (Deb et al., 2002). In this study, the NSGA-II was used with a TRNSYS simulation project.

SIMULATION

The goal of this study is providing Pareto curves by using simulation-based BHE sizing combined with Multi-opt 2. The Multi-opt 2 is a multicriteria optimization program by using the NSGA-II. This may give several solutions for decision makers to select one of them according to their desires. The followings are about simulation conditions.

Building & Ground

The target building of this case study is a residential complex located in Seoul, Korea. The total number of apartments is 493, of which 307 apartments have 59 m² floor area for each and 186 apartments have 72 m². Table 1 presents the hourly building and ground peak loads for each month. The total peak heating load is 1,172 kW found in January, and peak cooling load is 1,164 kW in

Table 1: Annual building peak load & ground peak load

Month	Hourly Peak Building Load(kW)		Hourly Peak Ground Load(kW)	
	Heating	**Cooling**	**Heating**	**Cooling**
January	1171.65	0	825.42	0
February	980.25	0	656.08	0
March	687.42	0	464.42	0
April	339.54	470.04	234.75	530.40
May	0	924.50	0	1093.03
June	0	1082.41	0	1287.05
July	0	1163.98	0	1390.21
August	0	1056.76	0	1263.99
September	0	1024.28	0	1205.17
October	0	704.58	0	819.49
November	734.44	163.69	505.79	193.58
December	979.48	0	667.28	0

Table 2: Building & ground properties

Parameters	**Values**
Building	
Floor area [m²]	59/72
Number of households	307/186
Boreholes	
Borehole spacing [m]	4/5/6
Number of boreholes	Optimizing
Borehole depth [m]	Optimizing
Header depth [m]	1
Design EWT [ºC]	30
Fluid specific heat [J/kg K]	3960
Borehole mass flow rate [kg/s]	0.2/unit
Pipe thermal conductivity [W/mK]	0.4
Grout thermal conductivity [W/mK]	2
Borehole radius [mm]	55
Borehole inner/outer radius [mm]	13/16
Center-to-center distance [mm]	47.1
Ground	
Thermal conductivity [W/mK]	2
Thermal diffusivity [m²/day]	0.08
Initial ground temperature [ºC]	10
Simulation period [year]	20

July. Using a plus sign for cooling and a minus one for heating, the ground loads can be calculated from the building loads and heat pump COPs as expressed in Equation (5).

$$Q_g = Q_b \times \left\{ \left(1 - \frac{1}{COP}\right) \times GT(Q_b, 0) + \left(1 + \frac{1}{COP}\right) \times LT(Q_b, 0) \right\} \quad (5)$$

Variable COPs of heat pump

For a sizing purpose, a mean heat pump COP has been used to calculate the ground loads simply and a priori. However, a heat pump cooling COP is to be decreased in reality, and a heating COP is increased during the long-term system operation. This COP variation affect a heat pump energy consumption. In addition, a heat pump energy consumption is directly connected to system operation cost. Therefore, variable COP must be used to deduce the Pareto curves. To account for the variable COPs in TRNSYS sizing simulations, an iteration process is required at every simulation time step. This is similar to the previous work (Ahmadfard et al., 2016).

Figure 5 shows the TRNSYS sizing simulation project, and the loop linking the components 3 to 5 in the figure shows the iteration step. The iteration starts from the component 3 to which the building load is inputted from the component 2. Simultaneously, the component 3 gets an initial EWT from the component 5 to calculate COP using Equation (6), where a_i and b_i mean the coefficients of cooling and heating, respectively.

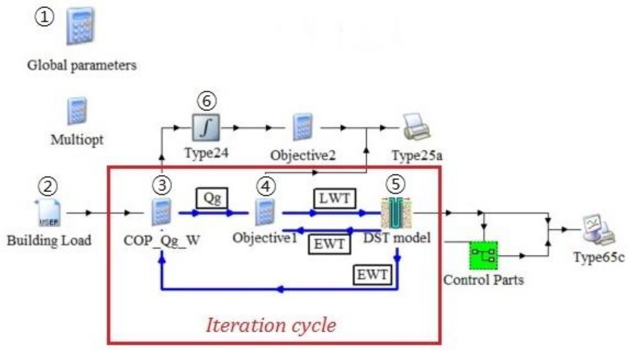

Figure 5: Iteration cycle of heat pump COP in TRNSYS.

Subsequently, the ground load (Q_g) is calculated at the component 3 by Equation (5), and this ground load is converted into a LWT (Leaving Water Temperature) from heat pumps by Equation (7). This iteration is repeated until convergence occurs. Properties used in simulations are given in Table 2. This variable COPs is also used for defining objective functions.

$$COP = (a_0 + a_1 EWT_{DST} + a_2 EWT_{DST}^2) \times GT(Q_b, 0) + (b_0 + b_1 EWT_{DST} + b_2 EWT_{DST}^2) \times LT(Q_b, 0) \quad (6)$$

$$LWT = EWT + \frac{Q_g}{\dot{m} \times c_p \times N} \quad (7)$$

Objective functions

The EWT_{DST} is a function of the BHE total length (L=N×H). Using this correlation, an optimization algorithm can calculate proper pairs of N and H to minimize the difference between EWT_{SET} and EWT_{DST}. Here, the first objective function is defined as Equation (8) considering where the ground load is cooling dominant or heating dominant.

$$\begin{gathered} \min \;\; F_{1,obj} = (\mathrm{EWT}_{DST,max} - \mathrm{EWT}_{c,set}) \times \mathrm{P} \\ + \\ (\mathrm{EWT}_{DST,min} - \mathrm{EWT}_{h,set}) \times (1 - \mathrm{P}) \\ \text{where,} \\ \mathrm{P} = +1 \;\; (\text{Cooling dominant pattern}) \\ \mathrm{P} = 0 \;\; (\text{Heating dominant pattern}) \end{gathered} \quad (8)$$

For instance, when the ground load is cooling dominant, the equation selects automatically the maximum EWT as a design EWT from a user-defined EWT range.

The second objective function is set to minimize the initial cost as Equation (9). Once users set a cost information (won/m or won/N) in the component 1, the initial cost is calculated by multiplying N, H, and the unit cost.

$$\min F_{2,obj} \; Initial \;\; cost = N \times H \times \text{cost} \;\; [₩] \quad (9)$$

The third objective function is given to minimize the heat pump energy consumption. The heat pump energy consumption can be derived from variable COPs and ground loads as expressed in Equation (10). The third objective function, the annual heat pump energy consumption, is defined as Equation (11), where the unit of *Period* is year. This is calculated in TRNSYS using the component 6.

$$W_{HP} = Q_g \times \left\{ \left(\frac{1}{1+COP} \right) \times GT(Q_b, 0) + \left(\frac{1}{1-COP} \right) \times LT(Q_b, 0) \right\} \qquad (10)$$

$$\min \; F_{3,obj} = \int_{t_1}^{t_2} W_{HP}\, dt \div (Period \times 10^3) \;\; [\mathrm{kW}] \qquad (11)$$

Design variables

In the multicriteria optimization, the algorithm search optimal values of design variables stochastically, within initially defined bounds and constraints of objective functions. If users set the population size and number of generation, the multi-opt 2 is run iteratively until the Pareto solutions are derived. Each population heads towards the Pareto-front.

A current population of inferior values proceeds to a next generation of superior values. Functionally, the population size represents the number of Pareto solutions, and the number of generations means the number of iterations.

The EWT affects the first objective function, $F_{1,obj}$ as well as the third objective function. In this study, the design variables of two objective function is set to *N* and *H*, consequently the EWT. All these design variables are declared as continuous variables, but the borehole spacing is ruled out in the optimization variables since some typical spacing values are used. Simulations are performed at pre-defined borehole spacing cases such as 4m, 5m, and 6m. Table 4 shows the constraints of design variables and parameters in the Multi-opt 2.

RESULTS

Simulations by the proposed method are run for the *L*-shape BHE configuration. A 3-dimensional graph is created since the three sets of objective functions are taken into account. Table 5 shows the result values of the final Pareto solutions, and Figure 6 to 8 show different projections by selecting two objective functions from the 3-dimensional graph.

Table 4: Design variables & Multi-opt parameters

Design variable	Constraint	
	Min	Max
N (number of boreholes)	40	85
H (borehole depth) [m]	230	300
Parameters	**Value**	
Population size	20	
Number of generations	10	
Crossing probability	0.7	
Mutation probability	0.1	

For this cooling dominant case, output values of EWT_{DST} is ranged between 24°C and 36°C in Table 5 which is determined by total length($N \times H$). Here, the total lengths present within the declared values in Table 4. From Table 5, the Pareto curves clearly appear to Figure 6 to 8. 4 m spacing appear the highest initial cost and lowest energy consumption since it has the longest length. And the energy consumption does not show noticeable differences in every case when the heat pump compression work only considered.

The higher EWT_{DST} is calculated, the higher heat pump energy consumption and the lower initial cost are obtained since the total length of BHEs is shorter. Each solution is linked to a set of variables (*B*, *N*, *H*, and EWT) and other objective functions (the annual heat pump energy and initial cost). From these Pareto solutions, decisions are made for example: If a project lacks the installation area for BHEs as shown in Figure 2, a limited number of boreholes (*N*) were selected with a short borehole spacing (*B*). Then, the decision maker can select a longer unit borehole depth (*H*). On the other hand, the decision maker may search for higher EWT_{DST} cases within acceptable lower COP ranges.

With a pre-defined single EWT_{SET}, the total length of BHEs tends to increase when the borehole spacing is small. As a result, the initial cost is increased, but the heat pump energy consumption is decreased. However, a small modification of the EWT_{SET} can largely reduce the initial cost as shown in Figure 8 while the increase in energy consumption is not noticeable. With the multi-objective sizing optimization tool, such information can be provided.

CONCLUSIONS AND FUTURE WORK

This study proposes a multi-objective BHE sizing method by using the Multi-opt 2 with NSGA-II. For the ground heat exchanger model, we select the DST model in TRNSYS. To simulate irregular bore field cases that are not accounted for with the DST model, a modification method is also proposed for *L*-shape borehole configurations.

The variable COP based sizing methods are used in this work for more detailed sizing and consequently for making Pareto solutions as a function of annual energy consumption.

Other than conventional sizing methods that use a single design EWT, the proposed multi-objective sizing method can provide various design solution to help decision making. Finally, in this study, a rule of thumb based modification method is used to describe irregular borehole configurations in the DST model. More detailed modification methods must be investigated in the future work.

Table 5: Results of Pareto solutions

B [m]	EWT_{DST} [°C]	N [m]	H [m]	Heat pump energy [kWh/a]	Total length [km]	Initial cost [KR won]
4	25.1	82	284.8	727,492	23.4	₩1,966,857,600
4	26.0	88	257.4	733,474	22.7	₩1,911,765,760
4	26.3	87	257.4	734,941	22.4	₩1,884,215,296
4	26.4	74	297.3	732,708	22.0	₩1,835,453,824
4	27.1	82	263.1	738,345	21.6	₩1,811,957,504
4	27.4	74	282.1	738,933	20.9	₩1,762,381,824
4	28.0	73	280.0	741,905	20.4	₩1,721,160,576
4	28.2	87	239.0	745,576	20.8	₩1,753,791,488
4	28.3	77	265.9	744,290	20.5	₩1,714,386,048
4	28.6	71	282.4	744,663	20.1	₩1,677,408,896
4	29.2	83	239.8	750,816	19.9	₩1,679,837,824
4	29.4	69	280.3	748,900	19.3	₩1,625,834,752
4	29.8	75	257.6	752,706	19.3	₩1,619,867,776
4	30.6	70	266.3	756,143	18.6	₩1,565,416,576
4	31.1	71	259.4	759,145	18.4	₩1,544,654,976
4	31.9	65	272.1	762,415	17.7	₩1,491,954,304
4	32.3	75	239.0	767,122	17.9	₩1,501,861,760
4	32.4	66	263.9	765,745	17.4	₩1,473,478,272
4	32.7	69	252.3	768,642	17.4	₩1,464,957,696
4	33.0	69	250.9	769,923	17.3	₩1,455,803,904
4	33.1	69	250.6	770,661	17.3	₩1,453,492,608
4	33.3	63	271.4	769,982	17.1	₩1,425,773,568
4	33.8	73	233.5	775,988	17.0	₩1,433,252,480
4	34.1	62	269.1	774,799	16.7	₩1,390,681,600
4	34.8	71	232.6	781,715	16.5	₩1,390,908,160
5	25.5	70	297.3	733,759	20.8	₩1,746,281,600
5	25.7	70	294.8	734,939	20.6	₩1,731,586,816
5	25.9	70	292.8	735,915	20.5	₩1,718,743,936
5	26.2	69	292.3	737,426	20.2	₩1,694,841,344
5	26.9	67	290.6	741,465	19.5	₩1,636,018,944
5	27.1	67	289.5	742,061	19.4	₩1,629,730,304
5	27.2	68	285.8	742,818	19.4	₩1,626,897,152
5	27.3	66	291.0	743,202	19.2	₩1,610,123,520
5	27.8	69	275.1	747,122	19.0	₩1,590,454,784
5	29.6	59	294.8	755,244	17.4	₩1,454,948,352
5	29.9	70	253.1	759,882	17.7	₩1,483,752,192
5	30.0	70	252.8	760,167	17.7	₩1,481,337,856
5	30.1	69	253.1	760,753	17.5	₩1,474,624,128
5	30.3	57	294.6	758,719	16.8	₩1,419,407,616
5	30.3	57	294.6	758,789	16.8	₩1,418,717,056
5	30.5	58	289.3	760,377	16.8	₩1,412,442,624
5	30.7	56	297.3	761,199	16.6	₩1,390,863,488
5	31.1	57	289.2	763,576	16.5	₩1,382,464,768
5	31.8	60	270.0	768,817	16.2	₩1,368,310,528
5	32.0	59	275.1	769,669	16.2	₩1,352,838,144
5	32.2	58	275.1	770,869	16.0	₩1,342,940,672
5	32.7	59	269.7	773,806	15.9	₩1,327,998,848
5	33.8	51	294.6	778,672	15.0	₩1,255,100,288
5	33.9	50	297.6	778,739	14.9	₩1,250,476,416
5	34.3	50	294.6	781,590	14.7	₩1,235,656,192
5	34.6	54	275.3	784,532	14.9	₩1,243,668,736
5	34.7	50	292.7	783,699	14.6	₩1,224,813,568
6	24.5	68	299.8	732,640	20.4	₩1,723,225,088
6	25.0	68	297.0	735,049	20.2	₩1,687,088,512
6	25.1	66	300.0	735,436	19.8	₩1,672,726,272
6	25.2	67	296.7	736,413	19.9	₩1,664,326,784
6	25.8	65	297.0	739,254	19.3	₩1,617,450,240
6	26.2	64	294.1	741,560	18.8	₩1,589,296,768
6	27.1	68	273.1	747,677	18.6	₩1,552,632,448
6	27.2	60	299.9	746,559	18.0	₩1,506,098,560
6	27.9	68	263.8	752,551	17.9	₩1,511,413,120
6	28.1	68	263.5	753,783	17.9	₩1,497,037,440
6	28.3	68	262.2	754,748	17.8	₩1,488,399,360
6	28.5	56	300.0	754,113	16.8	₩1,415,521,152
6	29.0	62	274.6	758,008	17.0	₩1,425,162,624
6	29.5	61	274.3	760,762	16.7	₩1,397,161,088
6	30.3	66	250.2	767,069	16.5	₩1,388,150,784
6	31.0	51	299.9	767,659	15.3	₩1,285,636,096
6	31.5	52	291.3	771,153	15.1	₩1,272,075,904
6	31.7	52	289.2	772,759	15.0	₩1,263,000,064
6	32.2	51	287.9	775,657	14.7	₩1,243,225,472
6	32.8	49	294.1	778,633	14.4	₩1,211,808,384
6	33.9	49	288.1	785,395	14.1	₩1,176,494,080
6	34.7	50	274.6	791,487	13.7	₩1,159,991,808

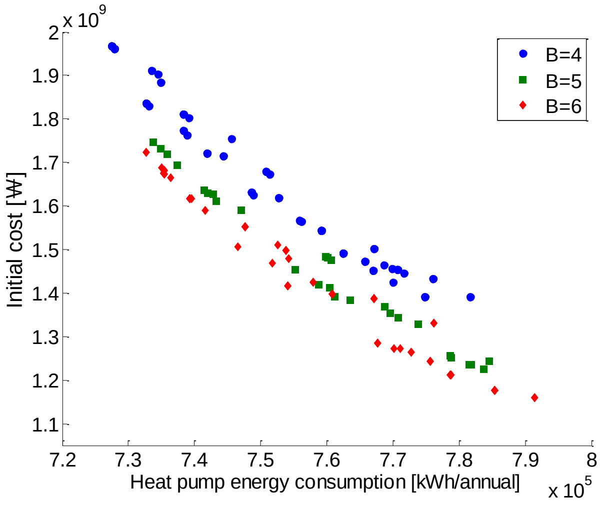

Figure 6: Heat pump energy consumption – Initial cost 2D projection.

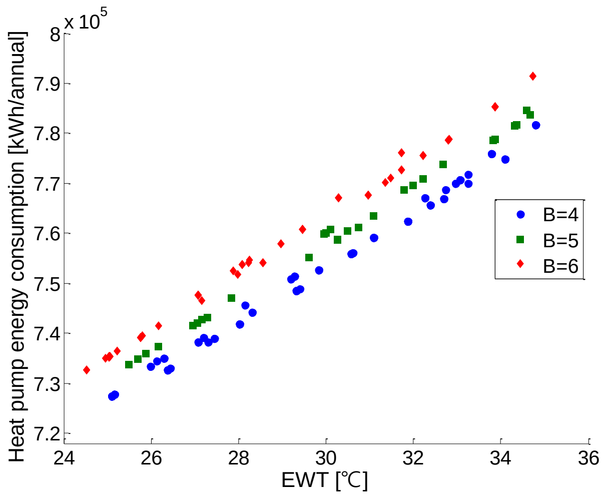

Figure 7: EWT – Heat pump energy consumption 2D projection.

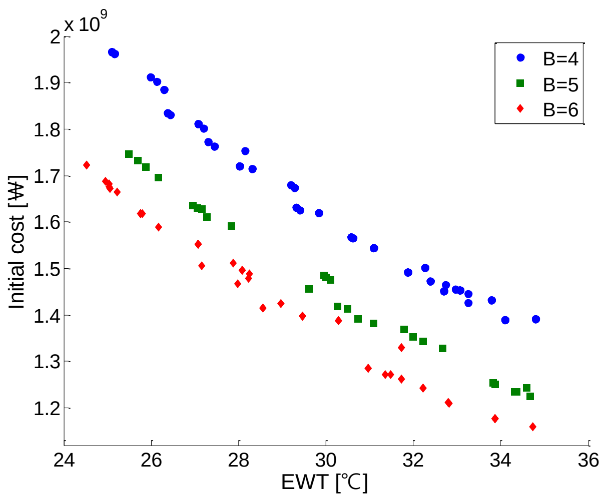

Figure 8: EWT – Initial cost 2D projection.

ACKNOWLEDGEMENTS

This work was supported by the National Research Foundation of Korea (NRF) grant funded by the Korea government (MSIP) (No. 2016R1C1B2011097).

NOMENCLATURE

B = Borehole spacing [m]

COP = Coefficient of performance

c_P = Specific heat [J/kg K]

EWT = Entering water temperature [°C]

F = Function

GT = Greater than

H = Borehole bured depth [m]

L = Total length of borehole [m]

LT = Less than

$\dot{m}$ = Mass flow rate [kg/h]

N = Number of boreholes

Q = Load [W]

R = Radius [m]

s = Number of bore field sides

V = Volume [m^3]

SUBSCRIPTS

b = Building

c = Cooling

DST = Duct Storage model

g = Ground

h = Heating

HP = Heat pump

max = Maximum

min = Minimum

obj = Objective

$modif$ = Modified

REFERENCES

Asadi, E., da Silva, M. G., Antunes, C. H., and Dias, L. (2012). A multi-objective optimization model for building retrofit strategies using TRNSYS simulations, GenOpt and MATLAB. *Building and Environment, 56*, 370-378.

Capozza, A., Zarrella, A., and De Carli, M. (2015). Analysis of Vertical Ground Heat Exchangers: The New CaRM Tool. Energy Procedia, 81, 288-297.

Deb, K. (2001). Multi-objective optimization using evolutionary algorithms. Vol. 16. John Wiley & Sons.

Deb, K., Pratap, A., Agarwal, S. and Meyarivan, T. A. M. T. (2002). A fast and elitist multiobjective genetic algorithm: NSGA-II. *IEEE transactions on evolutionary computation, 6*(2), 182-197.

E, J, Kim., M, Bernier., O, Cauret. and J, J, Roux. (2014). A hybrid reduced model for borehole heat exchangers over different time-scales and regions. *Energy, 77*, 318-326.

F, P, Chantrelle., H, Lahmidi., W, Keilholz., M, El, Mankibi and P, Michel. (2011). Development of a multicriteria tool for optimizing the renovation of buildings. *Applied Energy, 88*(4), 1386-1394.

Goldberg, D, E. (1989). Genetic algorithms in search, optimization, and machine learning. *Addion wesley 1989*: 102.

Hellström, G. (1989). Duct ground heat storage model, manual for computer code. Department of Mathematical Physics, University of Lund, Sweden.

Holland, J. H. (1975). Adaptation in natural and artificial systems: an introductory analysis with applications to biology, control, and artificial intelligence. *U Michigan Press.*

Kavanaugh, S. (1995). A design method for commercial ground-coupled heat pumps. *Transactions-American Society of Heating Refrigerating and Air conditioning Engineers 101*: 1088-1094.

L, Magnier. and F, Haghighat. (2010). Multiobjective optimization of building design using TRNSYS simulations, genetic algorithm, and Artificial Neural Network. *Building and Environment 45*.3: 739-746.

M, Ahmadfard., M, Bernier., M, Kummert. (2016). Evaluation of the design length of vertical geothermal boreholes using annual simulations combined with GenOpt. *Proceeding of the eSim 2016 Building Performance Simulation Conference*, May 3-6, 46-56.

M, Wetter. (2001). GenOpt - A generic optimization program. *Seventh International IBPSA Conference*, August 13-15.

S, Bertagnolio., M, Bernier. and M, Kummert. (2012). Comparing vertical ground heat exchanger models. *Journal of Building Performance Simulation*, Vol. 5, No. 6, 369–383.

S, H, Park., B, G, Jeon., Y, Kim., Y, S, Jang., E, J, Kim., (2016). A study on the simulation-based sizing of ground heat exchangers. *IAQVEC 2016, 9th International Conference on Indoor Air Quality Ventilation & Energy Conservation In Buildings*, October 23-26, 1482.